Chapter 12
Monotonic Strength and Fracture

In this chapter we describe the monotonic strength and fracture behavior of fiber reinforced composites at ambient temperatures. The term *monotonic behavior* means behavior under an applied stress that increases in one direction, i.e., not a cyclic loading condition. We discuss the behavior of composites under fatigue or cyclic loading as well as under conditions of creep in Chap. 13.

12.1 Tensile Strength of Unidirectional Fiber Composites

In Chap. 10 we discussed the prediction of elastic and thermal properties when the properties of the components are known. A particularly simple but crude form of this is the rule-of-mixtures, which works reasonably well for predicting the longitudinal elastic constants. Unfortunately, the same cannot be said for the strength of a fiber reinforced composite. It is instructive to examine why the rule-of-mixtures approach does not always work for strength properties of a composite. For a composite containing continuous fibers, unidirectionally aligned and loaded in the fiber direction (isostrain condition), we can write for the stress in the composite

$$\sigma_c = \sigma_f V_f + \sigma_m (1 - V_f), \tag{12.1}$$

where σ is the axial stress, V_f is the volume fraction, and the subscripts c, f, and m refer to composite, fiber, and matrix, respectively. The important question here is: What is the value of the matrix stress, σ_m? Ideally, it should be the in situ value of the stress on the matrix at a given strain. The main reason that the rule-of-mixtures does not always work for predicting the strength of a composite, while it works reasonably well for Young's modulus in the longitudinal direction, is that the elastic modulus is a relatively microstructure-insensitive property, while strength is a highly microstructure-sensitive property. For example, the grain size of a polycrystalline material affects its strength but not its modulus. Thus, the response of a composite for elastic modulus is nothing but the volume-weighted average of the

K.K. Chawla, *Composite Materials: Science and Engineering*,
DOI 10.1007/978-0-387-74365-3_12,

individual responses of the isolated components. Because the strength is an extremely structure-sensitive property, synergism can occur in regard to composite strength. Consider the various factors that may influence the composite strength properties. First, matrix or fiber structure may be altered during fabrication. Second, composite materials consist of two components whose thermomechanical properties are generally quite different and thus may have residual stresses and/or undergo structure alterations owing to these internal stresses. We discussed at length in Chap. 10 the effects of differential contraction during cooling from the fabrication temperature to ambient temperature, which leads to thermal stresses large enough to deform the matrix plastically, which leads to high dislocation density and work-hardening of the matrix (Chawla and Metzger 1972; Chawla 1973a, b; Arsenault and Fisher 1983; and Vogelsang et al. 1986).

Yet another source of microstructural modification of a component is a phase transformation induced by the fabrication process. In a metallic laminate composite made by roll-bonding aluminum and austenitic stainless steel (type 304), it was observed that the fabrication procedure work-hardened the steel and partially transformed the austenite to martensite (Chawla et al. 1986).

The matrix stress state may also be influenced by rheological interaction between the components during straining (Ebert and Gadd 1965; Kelly and Lilholt 1969). The plastic constraint on the matrix owing to the large differences in the Poisson's ratios of the matrix and the fiber, especially in the stage wherein the fiber deforms elastically while the matrix deforms plastically, can considerably alter the stress state in the composite. Thus, microstructural changes in one or both of the components, or rheological interaction between the components during straining can lead to the phenomenon of synergism in the strength properties. In view of this, the rule-of-mixtures should be regarded, in the best of circumstances, as an order of magnitude indicator of the strength of a composite.

12.2 Compressive Strength of Unidirectional Fiber Composites

Fiber reinforced composites under compressive loading can be regarded, as a first approximation, as elastic columns under compression. Thus, the main failure modes in the failure of a composite are the ones that occur in the buckling of columns. Buckling occurs when a slender column under axial compression becomes unstable against lateral movement of the central portion. The critical stress corresponding to failure by buckling of a column with ends-pinned is given by the Euler bucking formula:

$$\sigma_c = \frac{\pi^2 E}{16}\left(\frac{d}{l}\right)^2, \tag{12.2}$$

where E is the elastic modulus, d is the diameter, and l is the length of the column. It is easy to see that a high aspect ratio (l/d) will result in a low σ_c. Of course, in a fiber

reinforced composite we do not load a fiber directly and the conditions of ends-pinned do not prevail. The main effect of different end conditions of the column is that the length of the column should be replaced with an effective length. In a composite, the matrix provides some stability in the lateral direction. Rosen (1965a) showed by means of photoelasticity that fiber reinforced composites fail by periodic buckling of the fibers, with the buckling wavelength being proportional to the fiber diameter. This is not surprising in view of the fact that in the analysis of a column on an elastic foundation, it is observed that the buckling wavelength depends on the column diameter. Figure 12.1 shows schematically the three situations: an unbuckled fiber composite, in-phase buckling, and out-of-phase buckling. The in-phase buckling of fibers involves shear deformation of the matrix. In such a case the composite strength in compression is proportional to the matrix shear modulus G_m; that is, $\sigma_c = G_m/V_m$, where V_m is the matrix volume fraction. For an isotropic matrix we have $G_m = E_m/2(1 + \nu_m)$, where E_m and ν_m are the matrix Young's modulus and Poisson's ratio, respectively. Thus,

$$\sigma_c = \frac{E_m}{2(1+\nu_m)V_m}. \tag{12.3}$$

Out-of-phase buckling of fibers involves transverse compressive and tensile strains. The compressive strength in such a case is proportional to the geometric mean of the fiber and matrix Young's moduli (Rosen 1965a):

$$\sigma_c = 2V_f\left(\frac{V_f E_m E_f}{3V_m}\right)^{1/2}, \tag{12.4}$$

where V and E denote the volume fraction and Young's modulus, respectively, and the subscripts f and m denote fiber and matrix, respectively.

From Eqs. (12.3) and (12.4), we can see that the two failure modes in compression have a different dependence on the moduli of the components, that is,

$$\begin{matrix} \sigma_c \propto (E_m E_f)^{1/2} & \text{out - of - phase} \\ \sigma_c \propto G_m & \text{in - phase} \end{matrix}. \tag{12.5}$$

Thus, if we were to put the same fiber in two different matrices (i.e., with different matrix moduli), we should be able to distinguish between these two compressive failure modes. Lager and June (1969) did just that with boron fibers in two different polymer matrices. An out-of-phase buckling mode predominated at low fiber volume fractions. At high fiber volume fractions, fibers exerted more influence on each other and a coupled or in-phase buckling mode prevailed. The approximate nature of Eqs. (12.7) and (12.8) is easy to see. Both imply that as $V_m \to 0$ (or $V_f \to 1$), $\sigma_c \to \infty$, that is, the fibers are infinitely strong. Of course, no fibers are infinitely strong. Fiber/matrix adhesion (Hancox 1975) and matrix yielding (Piggott and Harris 1980) also affect the compressive strength of fiber composites. Narayanan and Schadler (1999) observed that the kink bands initiated

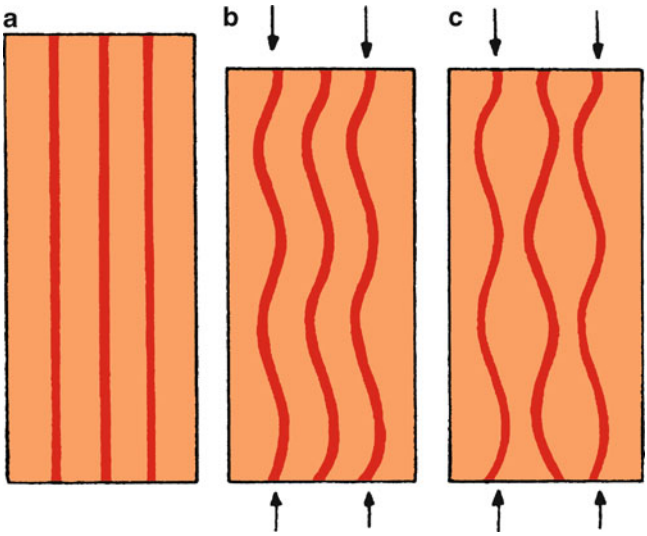

Fig. 12.1 (**a**) Unbuckled fiber composite, (**b**) in-phase buckling of fibers, and (**c**) out-of-phase buckling of fibers

from a damage zone comprising crushed and broken fibers. When the damage zone reached a critical size, the unsupported column of matrix caused a local matrix shear instability (or microbuckling). This local instability propagated as a kink band. The damage zone angle was found to depend on the interface properties, and it affected the strain to form kink bands. In the case of a laminated composite, poor interlaminar bonding can result in easy buckling of fibers (Piggott 1984). Kyriakides et al. (1995) investigated the failure in compression of unidirectionally reinforced AS4 carbon fiber/PEEK matrix composites. The failure load of the composite depended on geometric imperfections such as fiber waviness, and failure occurred via formation of kink bands. They modeled the composite as a two-dimensional solid with alternating fiber and matrix layers and investigated numerically the response in compression with different imperfections of various spatial distributions. The calculated responses were characterized by an initially elastic regime that ended at a limit load instability (the instability or limit load is the peak point on the system's load deflection curve), following which the deformation localized into inclined bands. As the localization process progressed, the fiber bending stresses at the ends of these bands grew to values comparable to those of the fiber strength. Heat and moisture as well as the ply stacking sequence can also affect the compressive strength. Budiansky and Fleck (1993) proposed a fiber microbuckling model which predicts a kinking stress as a function of the shear modulus of the composite, shear yield strain, and the strain hardening exponent. Gupta and coworkers (Gupta et al. 1994; Anand et al. 1994; Grape and Gupta 1995a, b) examined the behavior under uniaxial and biaxial compression of laminated carbon/carbon and carbon/polyimide composites. Carbon/carbon

laminates under uniaxial stress showed the formation of a diagonal shear fault, which consisted of a mixture of fiber bundle kinks and interply delaminations. Carbon/polyimide composites under inplane biaxial loading showed a new failure mechanism where the shear in the off-axis plies led to axial interply delaminations which were very similar to wing cracks observed in deformation of brittle materials under compression. Compressive strength of MMCs is generally higher than that of PMCs. Dève (1997) observed a compressive strength $\geq$4 GPa for aluminum alloy matrix containing high fiber volume fraction (55–65 %) Nextel 610 alumina fibers. Fiber microbuckling was the observed failure mode. For a review of various models and experimental techniques related to compressive failure of fiber reinforced composites, see Schultheisz and Waas (1996) and Waas and Schultheisz (1996).

12.3 Fracture Modes in Composites

A large variety of deformation modes can lead to failure of the composite. The operative failure mode depends, among other things, on loading conditions and the microstructure of a particular composite system. By *microstructure*, we mean fiber diameter, fiber volume fraction, fiber distribution, and damage resulting from thermal stresses that may develop during fabrication and/or in service. In view of the fact that many factors can and do contribute to the fracture process in composites, it is not surprising that a multiplicity of failure modes is observed in a given composite system.

12.3.1 Single and Multiple Fracture

In general, the fiber and matrix will have different values of strain at fracture. When the component that has the smaller breaking strain fractures, for example, a brittle fiber or a brittle ceramic matrix, the load carried by this component is thrown onto the other one. If the component with a higher strain of fracture can bear this additional load, the composite will show multiple fracture of the brittle component. A manifestation of this phenomenon is fiber bridging of the ceramic matrix (see Chap. 7). Eventually, a particular transverse section of the composite becomes so weak that the composite is unable to carry the load any further and it fails.

Consider the case of a fiber reinforced composite in which the fiber fracture strain is less than that of the matrix, for example, a ceramic fiber in a metallic matrix. The composite will then show a single fracture (Hancox 1975) when

$$\sigma_{\mathrm{fu}} V_{\mathrm{f}} > \sigma_{\mathrm{mu}} V_{\mathrm{m}} - \sigma'_{\mathrm{m}} V_{\mathrm{m}}, \tag{12.6}$$

where σ'_m is the matrix stress corresponding to the fiber fracture strain and σ_{fu} and σ_{mu} are the ultimate tensile stresses of the fiber and matrix, respectively. Equation (12.6) states that when the fibers break, the matrix will not be able to support the additional load. This is commonly the case with composites containing a large volume fraction of brittle fibers in a ductile matrix. All the fibers break in more or less one plane and the composite also fails in that plane.

If we have a composite that satisfies the condition

$$\sigma_{fu} V_f < \sigma_{mu} V_m - \sigma'_m V_m \tag{12.7}$$

then the fibers will break into small segments until the matrix fracture strain is reached.

In the case where the fibers have a fracture strain greater than that of the matrix (e.g., a ceramic matrix reinforced with ductile fibers), we will have multiple fractures in the matrix. We can write the expression for this as (Hale and Kelly 1972)

$$\sigma_{fu} V_f < \sigma_{mu} V_m + \sigma'_f V_f, \tag{12.8}$$

where σ'_f is the stress in the fiber at the matrix fracture strain. Figure 12.2 shows schematically the conditions for single and multiple fracture in fiber reinforced composites under tension. Single fracture occurs to the left of cross-over point, multiple fracture to the right. This will apply for matrix having a greater strain at fracture than the fiber.

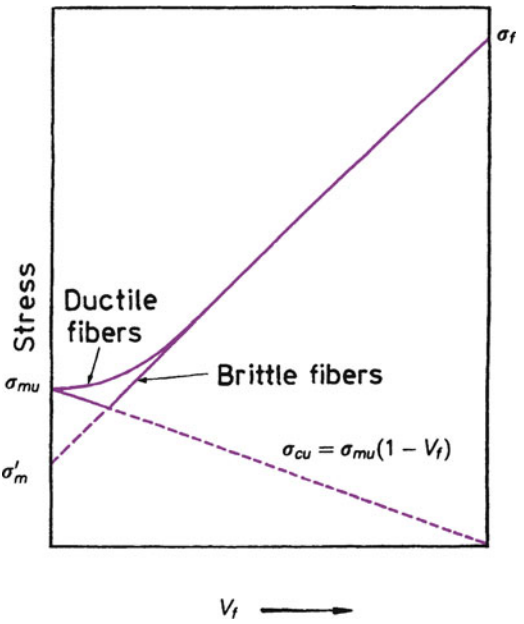

Fig. 12.2 Strength of the composite vs. fiber volume fraction for a composite with matrix having a greater strain at fracture than the fiber. Single fracture occurs to the left of cross-over point, multiple fracture occurs to the right

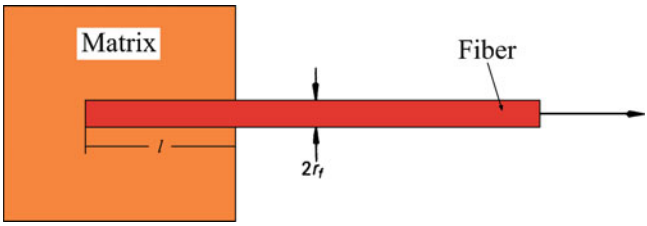

Fig. 12.3 A fiber of length l, embedded in a matrix, being pulled out

12.3.2 Debonding, Fiber Pullout, and Delamination Fracture

Debonding of the fiber/matrix interface, fiber pullout, and delamination fracture are some of the features that are commonly observed in fiber reinforced composites; these modes of fractue are not observed in conventional, monolithic materials. Consider the situation wherein a crack originates in the matrix and approaches the fiber/matrix interface. In a short fiber composite with a critical length l_c, fibers with extremities within a distance $l_c/2$ from the plane of the crack will debond and pull out of the matrix (see Fig. 10.7). These fibers will not break. In fact, the fraction of fibers pulling out will be l_c/l. Continuous fibers ($l > l_c$) invariably have flaws distributed along their length. Thus, some of them may fracture in the plane of the crack, while others may fracture away from the crack plane. This is treated in some detail later in this section.

The final fracture of the composite will generally involve some fiber pullout. Consider a model composite consisting of a fiber of length l embedded in a matrix; see Fig. 12.3. If this fiber is pulled out, the bonding between the matrix and the fiber will produce a shear stress τ parallel to the fiber surface. The shear force acting on the fiber as a result of this stress is given by $2\pi r_f \tau l$, where r_f is the fiber radius. Let τ_i be the maximum shear stress that the interface can support and let σ_{fu} be the fiber fracture stress in tension. The maximum force caused by this normal stress on the fiber is $\pi r_f^2 \sigma_{fu}$. For maximum fiber strengthening, we would like the fiber to break rather than get pulled out of the matrix. From a toughness point of view, however, fiber pullout may be more desirable. We can then write from the balance of forces the following condition for the fiber to be fractured under tension:

$$\pi r_f^2 \sigma_{fu} < 2\pi r_f \tau_i l$$

or

$$\frac{\sigma_{fu}}{4\tau_i} < \frac{l}{2r_f} = \frac{l}{d}, \tag{12.9}$$

where d is the fiber diameter and the ratio l/d is the aspect ratio of the fiber.

On the other hand, for fiber pullout to occur, we can write

$$\frac{l}{d} \leq \frac{\sigma_{\mathrm{fu}}}{4\tau_{\mathrm{i}}}. \tag{12.10}$$

The equality in this expression gives us the critical fiber length l_{c} for a given fiber diameter. Thus,

$$\frac{l_{\mathrm{c}}}{d} = \frac{\sigma_{\mathrm{fu}}}{4\tau_{\mathrm{i}}}. \tag{12.11}$$

This equation provides us with a means of obtaining the interface strength, namely, by embedding a single fiber in a matrix and measuring the load required to pull the fiber out. The load–displacement curve shows a peak corresponding to debonding, followed by an abrupt fall and wiggling about a constant stress level. Note that Eq. (12.11) gives l_{c}/d to be half that given by Eq. (10.77). This is because in the present case the fiber is being loaded from one end only.

A point that has not been mentioned explicitly so far is that real fibers do not have uniform properties but rather show a statistical distribution. Weak points are distributed along the fiber length. We treat these statistical aspects of fiber strength in detail in Sect. 12.4. Suffice it to say that it is more than likely that a fiber would break away from the main fracture plane. Interfacial debonding occurs around the fiber breakpoint. The broken fiber parts are pulled out from their cylindrical holes in the matrix during further straining. Figure 12.4a shows schematically the fiber pullout in a continuous fiber composite, while a practical example of fiber pullout in a boron fiber/aluminum matrix is shown in Fig. 12.4b. Work is done in the debonding process as well as in fiber pullout against frictional resistance at the interface. Outwater and Murphy (1969) showed that the maximum energy required for debonding is given by

$$W_{\mathrm{d}} = \left(\frac{\pi d^2}{24}\right)\left(\frac{\sigma_{\mathrm{fu}}^2}{E_{\mathrm{f}}}\right)x, \tag{12.12}$$

where x is the debond length.

This phenomenon of fiber pullout is very important in regard to toughness (Cottrell 1964). The fiber length l should be large but close to l_{c} for maximizing the fiber pullout work and to prevent the composite from separating into two halves. It should be recognized at the same time that for $l < l_{\mathrm{c}}$, the fiber will not get loaded to its maximum possible strength level and thus full fiber strengthening potential will not be realized.

We can estimate the work done in pulling out an isolated fiber in the following way (Fig. 12.4c). Let the fiber be broken a distance k below the principal crack plane, where $0 < k < l_{\mathrm{c}}/2$. Now let the fiber be pulled out through a distance x against an interfacial frictional shear stress, τ_{i}. Then the total force at that instant on the debonded fiber surface, which is opposing the pullout, is $\tau_{\mathrm{i}}\pi d(k - x)$. When the fiber is further pulled out a distance $\mathrm{d}x$, the work done by this force is $\tau_{\mathrm{i}}\pi d(k - x)\mathrm{d}x$.

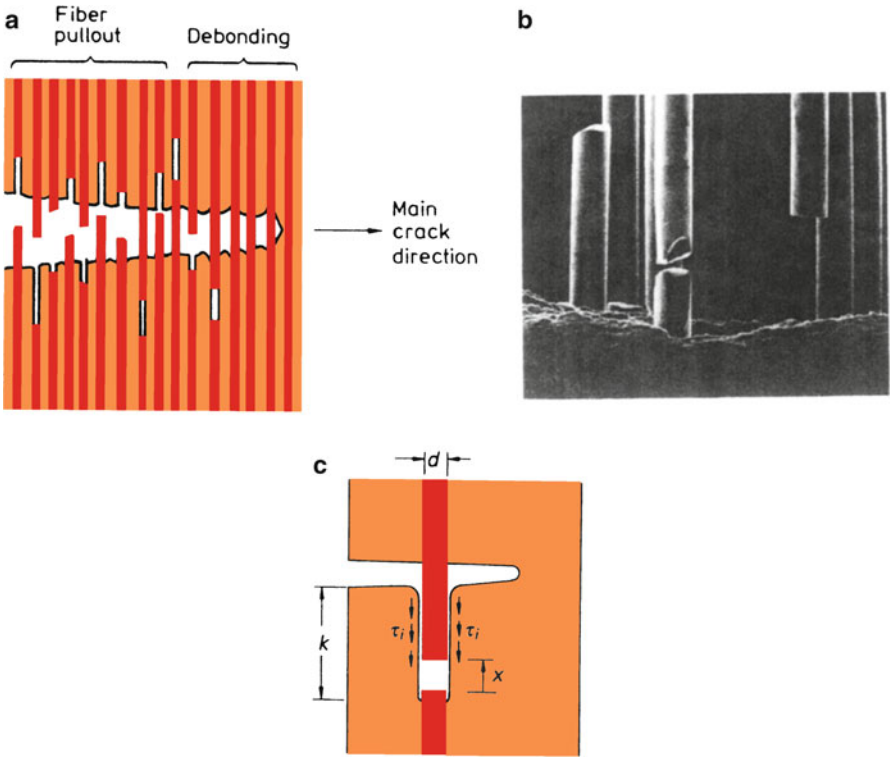

Fig. 12.4 (**a**) Schematic of fiber pullout in a continuous fiber composite. (**b**) Fiber pullout in a B/Al system. (**c**) Schematic of an isolated fiber pullout through a distance x against an interfacial shear stress, τ_i

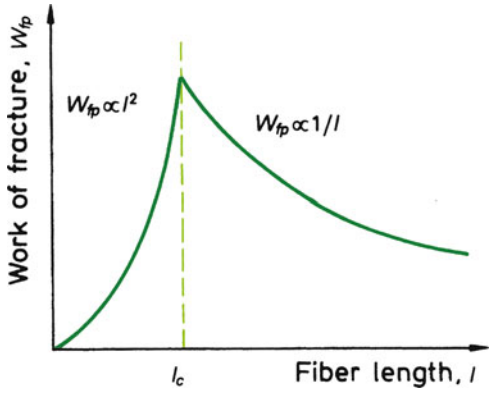

Fig. 12.5 Variation of work done in fiber pullout with fiber length

We can obtain the total work done in pulling out the fiber over the distance k by integrating. Thus,

$$\text{Work of fiber pullout} = \int_0^k \tau_i \pi d(k-x)\mathrm{d}x = \frac{\tau_i \pi d k^2}{2}. \tag{12.13}$$

The reader should be careful with our use of d as a symbol for the fiber diameter and differentiation. Now the pullout length of the fiber can vary between a minimum of 0 and a maximum of $l_c/2$. The average work of pullout per fiber is then

$$W_{fp} = \frac{1}{l_c/2}\int_0^{l_c/2} \frac{\tau_i \pi d k^2}{2}\mathrm{d}k = \frac{\tau_i \pi d {l_c}^2}{24}.$$

This analysis assumes that all fibers are pulled out. In a discontinuous fiber composite, it has been observed experimentally (Kelly 1970) that only the fibers with ends within a distance $l_c/2$ of the main fracture plane and that cross this fracture plane undergo pullout. Thus, it is more likely that a fraction (l_c/l) of fibers will pull out. The above expression for average work done per fiber can then be modified as

$$W_{fp} = \left(\frac{l_c}{l}\right)\frac{\pi d \tau_i l_c^2}{24}. \tag{12.14}$$

In general, fiber pullout provides a more significant contribution to composite fracture toughness than fiber/matrix debonding. The reader should appreciate the fact that debonding must precede pullout. Figure 12.5 shows schematically the variation of work of fracture with fiber length. For $l < l_c$, W_{fp} increases as l^2 (substitute l for k in Eq. (12.14)). Physically, this makes sense because as the fiber length increases, an increasing fiber length will be pulled out. For $l > l_c$, as pointed out earlier, some fibers will fracture in the plane of fracture of the composite and thus their contribution to W_{fp} will be nought. Those fibers whose ends are within a distance of $l_c/2$ from the fracture plane, they will undergo the process of fiber pullout. In this case, the average work of fracture is given by Eq. (12.14), i.e., W_{fp} varies as $1/l$ because with increasing fiber length, fiber breaks intervene and the fiber pullout decreases. The work of fracture, W_{fp} peaks at $l = l_c$. The reader can easily show that for $l = l_c$, the average stress in the fiber will only be half that in an infinitely long fiber.

One measure of fracture toughness can loosely be defined as resistance to crack propagation. Consider a fiber reinforced composite containing a crack transverse to the fibers. In such a situation, we can increase the crack propagation resistance by one of the following means, each of which involves additional work:

1. Plastic deformation of the matrix (applicable in a metal matrix).
2. Presence of weak interfaces, fiber/matrix separation, and deflection of the crack.
3. Fiber pullout.

For a metal matrix composite the work of fracture is mostly the work done during plastic deformation of the matrix. The work of fracture is proportional to $d(V_m/V_f)^2$ (Cooper and Kelly 1967), where d is the fiber diameter and V_m and V_f are the matrix and fiber volume fractions, respectively. This is understandable inasmuch as in the case of large-diameter fibers, for a given V_f, the advancing crack will result in a greater amount of plastically deformed matrix, which will result in a larger work of fracture.

Crack deflection along an interface frequently follows separation of the fiber/matrix interface. This provides us with a potent mechanism of increasing the crack propagation resistance in composites; we discussed this topic in Chap. 7. This improvement in fracture toughness owing to the presence of weak interfaces has been confirmed experimentally. This crack deflection mechanism can be a major source of toughness in ceramic matrix composites (Chawla 2003). Yet another related failure mode in laminated composites is the delamination failure associated with the plies and the fiber/matrix interface. This fracture mode is of importance in structural applications involving long-term use, for example, under fatigue conditions and where environmental effects are important. Highly oriented fibers such as aramid can also contribute to the work of fracture. Figure 12.6 shows a delamination-type fracture in a Kevlar aramid/epoxy composite (Saghizadeh and Dharan 1985) and the characteristic fibrillation of the Kevlar fiber, which stems

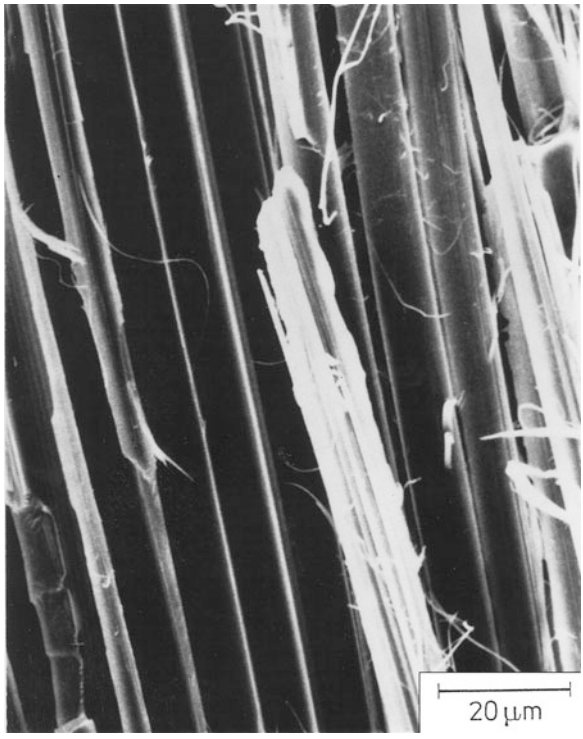

Fig. 12.6 A delamination-type fracture of Kevlar/epoxy composite. Note the characteristic fibrils in the fiber [from Saghizadeh and Dharan (1985), used with permission]

from its structure as described in Chap. 2. Carbon/epoxy composites, when tested for delamination fracture, showed clean exposed fiber surfaces (Saghizadeh and Dharan 1985).

Fiber pullout increases the work of fracture by causing a large deformation before fracture. In this case, the controlling parameter for work of fracture is the ratio d/τ_i, where d is the fiber diameter and τ_i is the interface shear strength. In the case of short fibers, the work of fracture resulting from fiber pullout also increases with the fiber length, reaching a maximum at l_c. In the case of continuous fibers, the work of fracture increases with an increase in spacing between the defects (Kelly 1971; Cooper 1970). Thus, one can increase the work of fracture by increasing the fiber diameter. This was discussed in Sect. 6.5 in regard to the toughness of metal matrix composites.

12.4 Effect of Variability of Fiber Strength

Most high-performance fibers are brittle. Thus, their strength must be characterized by a statistical distribution function. Figure 12.7a shows the strength distribution for a material that shows a large statistical variation in strength, while Fig. 12.7b shows an example of the strength of material in which the variability of strength is insignificant. We can safely put most metallic fibers or wires in the latter category. Most high-strength and high-stiffness fibers (aramid, polyethylene, B, C, SiC, Al_2O_3, etc.), however, follow some kind of statistical distribution of strength such as the one shown in Fig. 12.7a.

There are many statistical distribution functions for the strength of a material. For brittle materials, a distribution function called the Weibull statistical distribution function (named after the Swedish engineer who first proposed it) has been found to characterize the strength fairly well. For high-strength fibers also, the Weibull treatment of strength has been found to be quite adequate (Coleman 1958). Here we follow the treatment, due to Rosen (1965a, b, 1983), of this fiber-strength variability and its effect on the properties of a fiber reinforced composite. We can express the dependence of fiber strength on its length in terms of the following distribution function:

$$f(\sigma) = L\alpha\beta\sigma^{\beta-1}\exp\left(-L\alpha\sigma^{\beta}\right), \tag{12.15}$$

where L is the fiber length, σ is the fiber strength, and α and β are statistical parameters. $f(\sigma)$, a probability density function, gives the probability that the fiber strength is between σ and $\sigma + d\sigma$.

We define the kth moment, M_k of a statistical distribution function as

$$M_k = \int_0^{\infty} \sigma^k f(\sigma)\mathrm{d}\sigma. \tag{12.16}$$

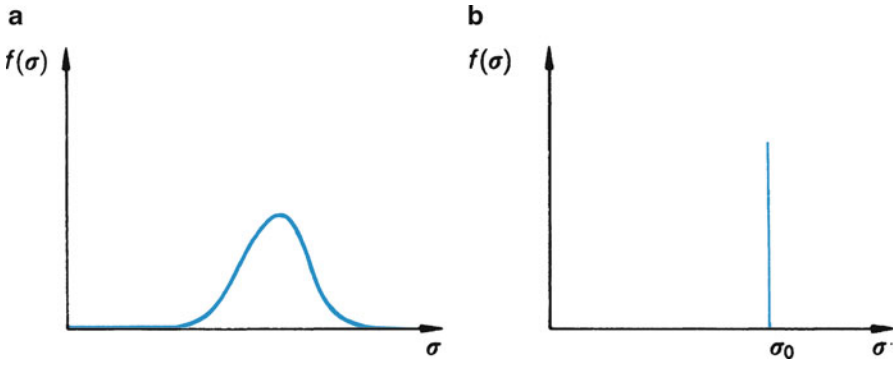

Fig. 12.7 (**a**) Strength distribution for a brittle material. (**b**) Strength distribution for material with insignificant variability of strength

Knowing that the mean strength of the fiber is given by $\bar{\sigma} = \int_0^\infty \sigma f(\sigma) \mathrm{d}\sigma$, we can write

$$\overline{\sigma} = M_1 \tag{12.17}$$

and the standard deviation s can be expressed as

$$s = \left(M_2 - M_1^2\right)^{1/2}. \tag{12.18}$$

From the Weibull distribution Eq. (12.15) and Eqs. (12.17) and (12.18), we obtain

$$\overline{\sigma} = (\alpha L)^{-1/\beta} \Gamma\left(1 - \frac{1}{\beta}\right) \tag{12.19}$$

and

$$s = (\alpha L)^{-1/\beta} \left[\Gamma\left(1 + \frac{2}{\beta}\right) - \Gamma^2\left(1 + \frac{1}{\beta}\right)\right]^{1/2}, \tag{12.20}$$

where $\Gamma(n)$ is the gamma function given by $\int_0^\infty \exp(-x) x^{n-1}\, \mathrm{d}x$. Note that x in this integral is a general, mathematical variable. The reader should not confuse x with the fiber length, x in Fig. 12.4. The coefficient of variation μ for this distribution then follows from the expression given below

$$\mu = \frac{s}{\overline{\sigma}} = \frac{\left[\Gamma(1 + 2/\beta) - \Gamma^2(1 + 1/\beta)\right]^{1/2}}{\Gamma(1 + 1/\beta)}. \tag{12.21}$$

We note that μ is a function only of the parameter β. Rosen showed that for $0.05 \leq \mu \leq 0.5$, $\mu \approx \beta^{-0.92}$ or $\mu \approx 1/\beta$. In other words, parameter β is an inverse measure of the coefficient of variation μ. For fibers that are characterized by the Weibull distribution (12.15), $\beta > 1$. For glass fibers, μ can be about 0.1, which would correspond to $\beta = 11$. For boron and SiC fibers, μ can be between 0.2 and 0.4 and β will be between 2.7 and 5.8.

Let us consider (12.19). We can write for a unit length of fiber

$$\overline{\sigma}_1 = k\alpha^{-1/\beta}, \tag{12.22}$$

where

$$k = \Gamma\left(1 + \frac{1}{\beta}\right). \tag{12.23}$$

For $\beta > 1$, we have $0.88 \leq k \leq 1.0$. Thus, we can regard the quantity $\alpha^{-1/\beta}$ as the reference strength level. We can plot Eq. (12.19) in the form of curves of $\overline{\sigma}/\alpha^{-1/\beta}$ (a normalized mean strength) against fiber length L for different β values, see Fig. 12.8. In Fig. 12.8, $\beta = \infty$ corresponds to a spike distribution function such as the one shown in Fig. 12.7b. In such a case, all the fibers have identical strength and there is no fiber length dependence. For $\beta = 10$, which corresponds to a $\mu \approx 12$ %, an order-of-magnitude increase in fiber length produces a 20 % fall in average strength. For $\beta = 4$, the corresponding fall in strength is about 50 %.

We can obtain the statistical mode σ^*, which is the most probable strength value by differentiating Eq. (12.15) and equating it to zero. Thus,

$$\sigma^* \approx \left(\frac{\beta - 1}{\beta}\right)^{1/\beta} (\alpha L)^{-1/\beta}. \tag{12.24}$$

For large β,

$$\sigma^* \approx (\alpha L)^{-1/\beta}. \tag{12.25}$$

$(\alpha L)^{-1/\beta}$, as mentioned earlier, is a reference stress level. The values of α and β can be obtained from experimental $\overline{\sigma}$ and μ values.

If we use Weibull statistics to characterize ceramic fibers, we can answer the following important question: For making tough, strong fiber reinforced ceramic matrix composites, would we want fibers with small or large Weibull modulus? Lara-Curzio et al. at Oak Ridge National Laboratory have examined this problem. Figure 12.9 shows their results in the form of fiber bundle strength vs. strain in a CMC for different Weibull modulus values. The take away message of this figure is that the higher the Weibull modulus of ceramic fibers, (i.e., the less uniformity in their properties), the more graceful failure of the CMC. It is understandable if we recall that a low Weibull modulus fiber will fracture in the composite at different strain values and thus spread the damage, which would lead to a final noncatastrophic failure of the CMC.

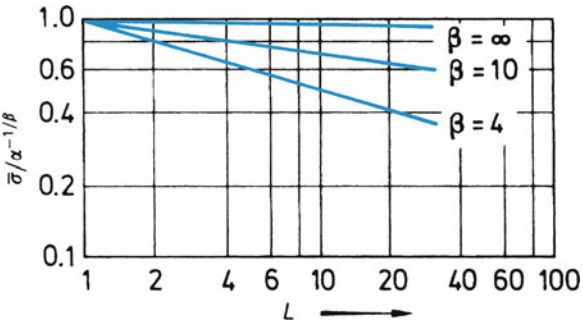

Fig. 12.8 Normalized mean fiber strength vs. fiber length L

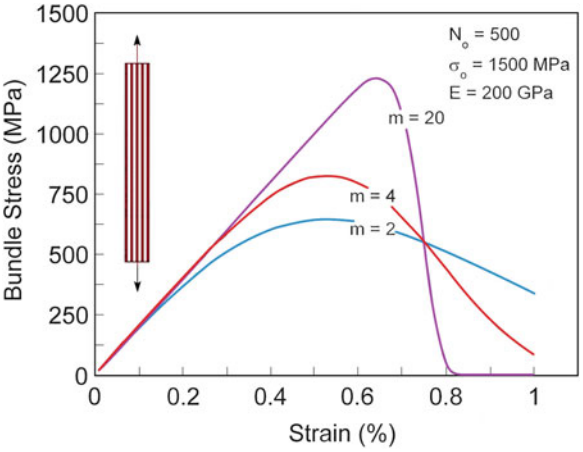

Fig. 12.9 Fiber bundle strength vs. strain in a CMC for different Weibull modulus values (courtesy of E. Lara-Curzio)

There is yet another important statistical point with regard to this variability of fiber strength. This has to do with the fact that in a unidirectionally aligned fiber composite, the fibers act in a bundle in parallel. It turns out that the strength of a bundle of fibers whose elements do not possess a uniform strength is not the average strength of the fibers. Coleman (1958) investigated this nontrivial problem, which we describe below.

In the simplest case, we assume that all fibers have the same cross section and the same stress–strain curve but with different strain-to-fracture values. Let the strength distribution function for the fiber be given by the Weibull function $f(\sigma)$, Eq. (12.15), then the probability that a fiber will break before a certain value σ is attained is given by the cumulative strength distribution function $F(\sigma)$. We can write

$$F(\sigma) = \int_0^{\sigma} f(\sigma)\mathrm{d}\sigma. \tag{12.26}$$

One makes a large number of measurements of strength of individual packets or bundles of fibers. Each bundle has the same large number of fibers of identical cross section and they are loaded from their extremities. From such tests we can obtain the mean fiber strength in the bundle. Daniels (1945) showed that, for a very large number of fibers in the bundle, the distribution of the mean fiber strength at bundle failure attains a normal distribution, with the expectation or mean value being given by

$$\overline{\sigma}_{\mathrm{B}} = \sigma_{\mathrm{fu}}[1 - F(\sigma_{\mathrm{fu}})], \tag{12.27}$$

where σ_{fu} is the maximum fiber strength, i.e., σ_{fu} corresponds to the condition where the bundle supports the maximum load. Thus, we can obtain σ_{fu} by taking the derivative and equating it to zero,

$$\frac{\mathrm{d}}{\mathrm{d}\sigma}\{\sigma[1 - F(\sigma)]\}_{\sigma=\sigma_{\mathrm{fu}}} = 0. \tag{12.28}$$

The fiber bundle strength, σ_{B} values are characterized by the following density function for normal distribution function:

$$\omega(\sigma_{\mathrm{B}}) = \frac{1}{\Psi_{\mathrm{B}}\sqrt{2\pi}} \exp\left[-\frac{1}{2}\left(\frac{\sigma_{\mathrm{B}} - \overline{\sigma}_{\mathrm{B}}}{\Psi_{\mathrm{B}}}\right)^2\right], \tag{12.29}$$

where Ψ_{B} is the standard deviation given by

$$\Psi_{\mathrm{B}} = \sigma_{\mathrm{fu}}\{F(\sigma_{\mathrm{fu}})[1 - F(\sigma_{\mathrm{fu}})]\}^{1/2} N^{-1/2}, \tag{12.30}$$

where N is the number of fibers in the bundle.

As N becomes very large, not unexpectedly, the standard variation Ψ_{B} becomes small. That is, the larger the number of fibers in the bundle, the more reproducible is the bundle strength. For bundles characterized by Eq. (12.29), we can define a cumulative distribution function $\Omega(\sigma_{\mathrm{B}})$. Thus,

$$\Omega(\sigma_{\mathrm{B}}) = \int_0^{\sigma_{\mathrm{B}}} \omega(\sigma_{\mathrm{B}})\mathrm{d}\sigma_{\mathrm{B}}. \tag{12.31}$$

Consider the Weibull distribution, Eq. (12.15), then we have [from Eq. (12.28)]

$$\sigma_{\mathrm{fu}} = (L\alpha\beta)^{-1/\beta}. \tag{12.32}$$

Substituting this in Eq. (12.27), we get the following expression (left as an exercise for the reader to do) for the mean fiber bundle strength

$$\overline{\sigma}_{\mathrm{B}} = (L\alpha\beta e)^{-1/\beta}. \tag{12.33}$$

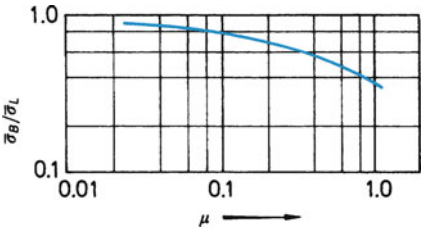

Fig. 12.10 Normalized fiber bundle strength vs. variance μ of the fiber population

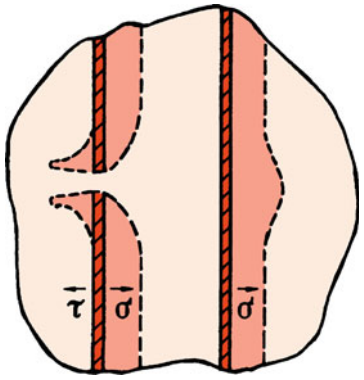

Fig. 12.11 Perturbation of stress state caused by a fiber break

In Eq. (12.33) e is the constant, called Euler's number, equal to 2.718. If we compare this mean fiber bundle strength value Eq. (12.33) to the mean value of the fiber strength obtained from equal-length fibers tested individually, Eq. (12.19), we note the following salient points. When there is no dispersion in fiber strength, i.e., all fibers show the same strength value, the mean bundle strength equals the mean fiber strength; see Fig. 12.10. As the coefficient of variation of fiber strength increases above zero, the mean bundle strength decreases and, in the limit of an infinite dispersion, tends to zero. For a 10 % variance, the mean bundle strength is about 80 % of the mean fiber strength, while for a variance of 25 %, the bundle strength is about 60 % of the mean fiber strength.

In view of the statistical distribution of fiber strength, it is natural to extend these ideas to composite strength. We present here the treatment due to Rosen (1965b, 1983). On straining a fiber reinforced composite, fibers (assuming that they are more brittle than the matrix) fracture at various points before a complete failure of the composite occurs. There occurs an accumulation of fiber fractures with increasing load. At a certain point, one transverse section will be weakened as a result of the statistical accumulation of fiber fractures, hence the name *cumulative weakening model of failure*. Because the fibers have nonuniform strength, it is expected that some fibers will break at very low stress levels. Figure 12.11 shows the perturbation in stress state when a fiber fracture occurs. At the point of fiber fracture, the tensile stress in the fiber drops to zero (see also Fig. 10.16). From this point the tensile stress in the fiber increases along the fiber length along the two

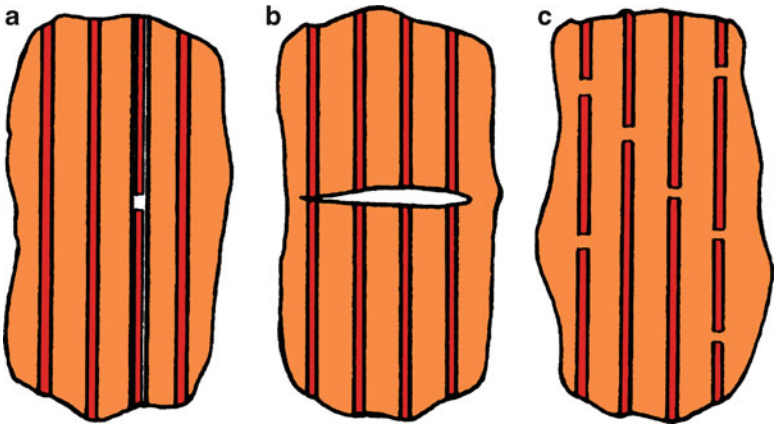

Fig. 12.12 Fracture models: (**a**) interface delamination where the composite acts as a fiber bundle, (**b**) first fiber fracture turns into a complete fracture, (**c**) cumulative damage—statistical

fiber segments as per the load transfer mechanism by interfacial shear described in Chap. 10. As a result, either the matrix would yield in shear or an interfacial failure would occur. Additionally, this local drop in stress caused by a fiber break will throw the load onto adjoining fibers, causing stress concentrations there (see Fig. 12.11). Upon continued straining, progressive fiber fractures cause a cumulative weakening and a redistribution of the load in the composite. Let us explore the different possibilities. After the first fiber fracture, the interfacial shear stresses may cause delamination between this broken fiber and the matrix, as shown in Fig. 12.11a. When this happens, the broken and delaminated fiber becomes totally ineffective and the composite behaves as a bundle of fibers. The second alternative is that a crack, starting from the first fiber break, propagates through the other fibers in a direction normal to the fibers; see Fig. 12.11b. Such a situation will occur only if the fiber and matrix are very strongly bonded and if the major component is very brittle. In the absence of these two modes, cumulative damage results. With increased loading, additional fiber fractures occur and a statistical distribution is obtained; see Fig. 12.11c.

Rosen (1983) considers in this model that the composite strength is controlled by a statistical accumulation of failures of individual volume elements that are separated by barriers to crack propagation; thus, these elements fail independently. The load on the matrix is ignored. Increased loading leads to individual fiber breaks at loads less than the ultimate fracture load of the composite. An individual fiber break does not make the whole fiber length ineffective, it only reduces the capacity of the fiber being loaded in the vicinity of fiber break. The stress distribution in the fiber is one of full load over its entire length less a length near the break over which the load is zero. This length is called the *ineffective length*. Thus, the composite is considered to be made up of a series of layers, each layer consisting of a packet of fiber elements embedded in the matrix. The length of each fiber element or the packet height is equal to the ineffective length.

As the load is increased, fiber breaks accumulate until at a critical load a packet of elements is unable to transmit the applied load and the composite fails. Thus, composite failure occurs because of this weakened section. A characteristic length δ corresponding to the packet height must be chosen. The term δ is defined as the length over which the stress attains a certain fraction ϕ of the unperturbed stress in the fiber. Rosen took ϕ equal to that length over which the stress increases elastically from 0 (at a fiber end) to 90 % of the unperturbed level. One then derives the stress distribution in the fiber elements and packets. The theory of the weakest link is then applied to obtain the composite strength. In the case of fibers characterized by the Weibull distribution, the stress distribution in the fiber elements is

$$w(\sigma) = \delta\alpha\beta\sigma^{\beta-1}\exp\left(-\delta\alpha\sigma^{\beta}\right), \tag{12.34}$$

where δ is the fiber element length (i.e., the ineffective length).

The composite is now a chain, the strength of whose elements is given by a normal distribution function $w(\sigma_B)$. The strength of a chain having m links (do not confuse with the Weibull modulus) of this population is characterized by a distribution function $\lambda(\sigma_c)$:

$$\lambda(\sigma_c) = mw(\sigma_c)[1 - \Omega(\sigma_c)]^{m-1}, \tag{12.35}$$

where

$$\Omega(\sigma_c) = \int_0^{\sigma_c} w(\sigma_c)\mathrm{d}\sigma. \tag{12.36}$$

Suppose now that the number of elements N (i.e., the number of fibers in the bundle) in a composite is so large that the standard deviation of the packet tends to zero. Then the statistical mode of composite strength is equal to $\overline{\sigma}_B$ Eq. (12.27).

In the case of a Weibull distribution, it follows from Eq. (12.33) that

$$\sigma_c^* = (\delta\alpha\beta e)^{-1/\beta} \tag{12.37}$$

and the statistical mode of the tensile strength of the composite is

$$\sigma^* = V_f(\delta\alpha\beta e)^{-1/\beta}, \tag{12.38}$$

where V_f is the fiber volume fraction and $e = 2.718$.

It should be pointed out that δ will be of the order of 10–100 fiber diameters and thus much smaller than the gage length used for individual tests.

If we compare the (cumulative) average strength of a group of fibers of length L with the expected fiber strength from Eqs. (12.21) and (12.37), we get

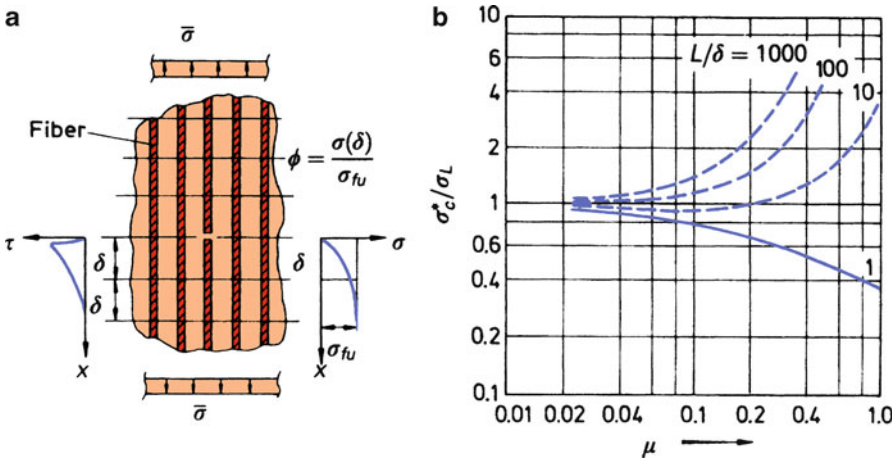

Fig. 12.13 Normalized composite strength $\sigma_c^*/\bar{\sigma}_L$ vs. variance μ (from Fiber composite materials, ASM, 1965, pp 39, 38, used with permission)

$$\frac{\sigma_c^*}{\bar{\sigma}_L} = \left(\frac{L}{\delta\beta e}\right)^{1/\beta} \frac{1}{\Gamma(1+1/\beta)}. \tag{12.39}$$

For $\beta = 5$ and $L/\delta = 100$, we have $\sigma_c^*/\bar{\sigma}_L = 1.62$; that is, the composite will be much stronger than what we expect from individual fiber tests. We can plot the composite strength σ_c^*, normalized with respect to the average strength $\bar{\sigma}_L$, of individual fibers of length L against μ, the variance of individual fiber strengths; see Fig. 12.13. The curves shown are for different values of the ratio L/δ. For $L/\delta = 1$, that is, the fiber length is equal to the ineffective length, the statistical mode of composite strength is less than the average fiber strength. This difference between the two increases with an increase in μ of the fibers. For a more realistic ratio, for example, $L/\delta > 10$, we note that the composite strength is higher than the average fiber strength.

A modification of this cumulative weakening model has been proposed by Zweben and Rosen (1970), which takes into account the redistribution of stress that results at each fiber break; that is, there is greater probability that fracture will occur in immediately adjacent fibers because of a stress magnification effect.

12.5 Strength of an Orthotropic Lamina

We saw in Chaps. 10 and 11 that fiber reinforced composites are anisotropic in elastic properties. This results from the fact that the fibers are aligned in the matrix. Additionally, the fibers are, generally, a lot stiffer and stronger than the matrix. Therefore, not unexpectedly, fiber reinforced composites also show anisotropy in strength properties. Quite frequently, the strength in the longitudinal direction is

as much as an order of magnitude greater than that in the transverse direction. It is of great importance for design purposes to be able to predict the strength of a composite under the loading conditions prevailing in service. The use of a failure criterion gives us information about the strength under combined stresses. We assume, for simplicity, that the material is homogeneous; that is, its properties do not change from point to point. In other words, we treat a fiber reinforced lamina as a homogeneous, orthotropic material (Rowlands 1985). We present below a brief account of different failure criteria.

12.5.1 Maximum Stress Theory

Failure will occur when any one of the stress components is equal to or greater than its corresponding allowable or intrinsic strength. Thus, failure will occur if

$$\begin{array}{ll} \sigma_1 \geq X_1^{\mathrm{T}} & \sigma_1 \leq -X_1^{\mathrm{C}} \\ \sigma_2 \geq X_2^{\mathrm{T}} & \sigma_2 \leq -X_2^{\mathrm{C}}, \\ \sigma_6 \geq S & \sigma_6 \leq S \end{array} \tag{12.40}$$

where X_1^{T} is the ultimate uniaxial tensile strength in the fiber direction, X_1^{C} is the ultimate uniaxial compressive strength in the fiber direction, X_2^{T} is the ultimate uniaxial tensile strength transverse to the fiber direction, X_2^{C} is the ultimate uniaxial compressive strength transverse to the fiber direction, and S is the ultimate planar shear strength. When any one of the inequalities indicated in Eq. (12.40) is attained, the material will fail by the failure mode related to that stress inequality. No interaction between different failure modes is permitted in this criterion. Consider an orthotropic lamina, that is, a unidirectional fiber reinforced prepreg subjected to a uniaxial tensile stress σ_x in a direction making an angle θ with the fiber direction. We then have, for the stress components in the 1–2 system,

$$\begin{bmatrix} \sigma_1 \\ \sigma_2 \\ \sigma_6 \end{bmatrix} = [T]_\sigma \begin{bmatrix} \sigma_x \\ \sigma_y \\ \sigma_s \end{bmatrix}, \tag{12.41a}$$

where

$$[T]_\sigma = \begin{bmatrix} m^2 & n^2 & 2mn \\ n^2 & m^2 & -2mn \\ -mn & mn & m^2 - n^2 \end{bmatrix}, \quad m = \cos\theta, \quad n = \sin\theta.$$

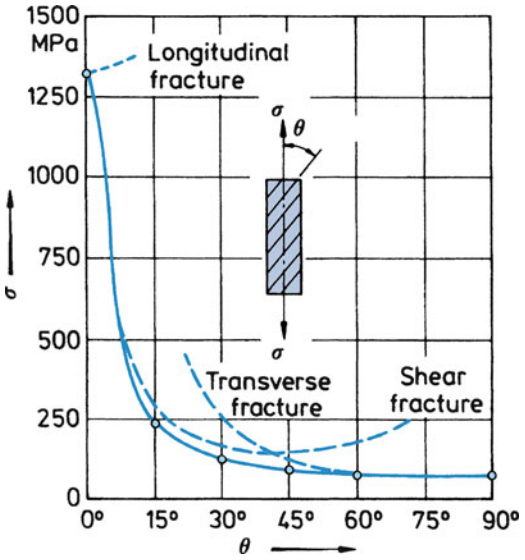

Fig. 12.14 Variation of strength with fiber orientation for boron/epoxy. Quadratic interaction criterion (*solid curve*) shows better agreement with experimental data than the maximum stress criterion (*dashed curve*) [after Pipes and Cole (1973)]

Using the fact that only σ_x is nonzero, we obtain

$$\begin{aligned} \sigma_1 &= \sigma_x m^2 \\ \sigma_2 &= \sigma_x n^2 \\ \sigma_6 &= -\sigma_x mn \end{aligned} \quad . \tag{12.41b}$$

Using these expressions for σ_x in conjunction with Eq. (12.40), we get, according to the maximum stress criterion, the following three independent failure modes:

$$\begin{aligned} \sigma_x &= \frac{X_1^{\mathrm{T}}}{m^2} \quad \text{(longitudinal tensile)} \\ \sigma_x &= \frac{X_2^{\mathrm{T}}}{n^2} \quad \text{(transverse tensile)} \\ \sigma_x &= \frac{S}{mn} \quad \text{(planar shear)} \end{aligned} \quad , \tag{12.42}$$

Here we are disregarding the sign of the shear stress, S. Figure 12.14 shows the failure stress with changing fiber orientation, θ. Note the failure mode changes from longitudinal tension to planar shear to transverse tension, as shown by the dashed lines. The agreement with experiment is poor, particularly around $\theta = \pi/4$. This indicates that at intermediate angles, interactions between failure modes do occur.

12.5.2 Maximum Strain Criterion

This criterion is analogous to the maximum stress criterion. Failure occurs when any one of the strain components is equal to or greater than its corresponding allowable strain. Thus,

$$\begin{aligned} \varepsilon_1 &\geq e_1^{\mathrm{T}} \quad \varepsilon_1 \leq -e_1^{\mathrm{C}} \\ \varepsilon_2 &\geq e_2^{\mathrm{T}} \quad \varepsilon_2 \leq -e_2^{\mathrm{C}} \\ \varepsilon_6 &\geq e_6 \quad \varepsilon_6 \geq e_6 \end{aligned}, \tag{12.43}$$

where e_1^{T} is the ultimate tensile strain in the fiber direction, e_1^{C} is the ultimate compressive strain in the fiber direction, e_2^{T} is the ultimate tensile strain in the transverse direction, e_2^{C} is the ultimate compressive strain in the transverse direction, and e_6 is the ultimate planar shear strain. This criterion is also not very satisfactory for the same reason as the maximum stress criterion, namely, absence of any interaction of failure modes.

12.5.3 Maximum Work (or the Tsai–Hill) Criterion

This criterion, originally proposed by Hill, is based on a modification of the distortion energy criterion for ductile metals. Hill's modification worked for anisotropic ductile metals such as metals that have undergone rolling etc. The Tsai–Hill criterion adopted Hill's modification to orthotropic fiber reinforced composites. According to the Tsai–Hill criterion, failure of an orthotropic lamina will occur under a general two-dimensional stress state when the following expression holds:

$$\frac{\sigma_1^2}{X_1^2} - \frac{\sigma_1\sigma_2}{X_1^2} + \frac{\sigma_2^2}{X_2^2} + \frac{\sigma_6^2}{S^2} \leq 1, \tag{12.44}$$

where X_1, X_2, and S are the longitudinal tensile failure strength, the transverse tensile failure strength, and the inplane shear failure strength, respectively. If compressive stresses are involved, then the corresponding compressive failure strengths should be used.

Consider again a uniaxial stress σ_x applied to an orthotropic lamina. Then, following Eq. (12.41), we can write

$$\begin{aligned} \sigma_1 &= \sigma_x m^2 \\ \sigma_2 &= \sigma_x n^2 \\ \sigma_6 &= -\sigma_x mn \end{aligned}, \tag{12.45}$$

where $m = \cos\theta$ and $n = \sin\theta$. Substituting these values in Eq. (12.44), we have

$$\frac{m^4}{X_1^2} + \frac{n^4}{X_2^2} + m^2n^2\left(\frac{1}{S^2} - \frac{1}{X_1^2}\right) < \frac{1}{\sigma_x^2} = \frac{1}{\sigma_\theta^2}. \tag{12.46}$$

This expression gives us the off-axis strength of composite lamina as function of fiber orientation. We can use this to verify the validity of the criterion. This criterion does take into account the interaction between the failure modes. However, it does not make any direct distinction between tensile and compressive stresses.

12.5.4 Quadratic Interaction Criterion

As the name indicates, this criterion takes into account the stress interactions. Tsai and Wu (1971) proposed this modification of the Hill theory for a lamina by adding some additional terms. Tsai and Hahn (1980) provide a good account of this criterion. According to this theory, the failure surface in stress space can be described by a function of the form

$$f(\sigma) = F_i\sigma_i + F_{ij}\sigma_i\sigma_j = 1 \qquad i,j = 1,2,6, \tag{12.47}$$

where F_i and F_{ij} are the strength parameters. For the case of plane stress, $i, j = 1$, 2, 6. We can expand Eq. (12.47) as follows:

$$\begin{aligned} &F_1\sigma_1 + F_2\sigma_2 + F_6\sigma_6 + F_{11}\sigma_1^2 + F_{22}\sigma_2^2 + F_{66}\sigma_6^2 + 2F_{12}\sigma_1\sigma_2 \\ &\quad + 2F_{16}\sigma_1\sigma_6 + 2F_{26}\sigma_2\sigma_6 = 1. \end{aligned} \tag{12.48}$$

For the orthotropic lamina, sign reversal for normal stresses, whether tensile or compressive, is important. The linear stress terms provide for this difference. For the shear stress component, the sign reversal should be immaterial. Thus, terms containing the first-degree shear stress must vanish. These terms are $F_{16}\sigma_1\sigma_6$, $F_{26}\sigma_2\sigma_6$, and $F_6\sigma_6$. The stress components in general are not zero. Therefore, for these three terms to vanish, we must have

$$F_{16} = F_{26} = F_6 = 0.$$

Equation (12.48) is now simplified to

$$F_1\sigma_1 + F_2\sigma_2 + F_{11}\sigma_1^2 + F_{22}\sigma_2^2 + F_{66}\sigma_6^2 + 2F_{12}\sigma_1\sigma_2 = 1. \tag{12.49}$$

There are six strength parameters in Eq. (12.49). We can measure five of these by the following simple tests.

12.5.4.1 Longitudinal (Tensile and Compressive) Tests

If $\sigma_1 = X_1^{\mathrm{T}}$, then $F_{11}\left(X_1^{\mathrm{T}}\right)^2 + F_1 X_1^{\mathrm{T}} = 1$.

If $\sigma_1 = -X_1^{\mathrm{C}}$, then $F_{11}\left(X_1^{\mathrm{C}}\right)^2 + F_1 X_1^{\mathrm{C}} = 1$.

From these we get

$$F_{11} = \frac{1}{X_1^{\mathrm{T}} X_1^{\mathrm{C}}} \tag{12.50}$$

and

$$F_1 = \frac{1}{X_1^{\mathrm{T}}} - \frac{1}{X_1^{\mathrm{C}}}. \tag{12.51}$$

12.5.4.2 Transverse (Tensile and Compressive) Tests

If X_2^{T} and X_2^{C} are the transverse tensile and compressive strengths, respectively, then proceeding as earlier, we get

$$F_{22} = \frac{1}{X_2^{\mathrm{T}} X_2^{\mathrm{C}}} \tag{12.52}$$

and

$$F_2 = \frac{1}{X_2^{\mathrm{T}}} - \frac{1}{X_2^{\mathrm{C}}}. \tag{12.53}$$

12.5.4.3 Longitudinal Shear Test

If S is the shear strength, we have

$$F_{66} = \frac{1}{S^2}. \tag{12.54}$$

Thus, we can express all the failure constants except F_{12} in terms of the ultimate intrinsic strength properties. F_{12} is the only remaining parameter and it must be evaluated by means of a biaxial test, which can be quite complicated to do. Many workers (Hoffman 1967; Cowin 1979) have proposed variations of the Tsai–Wu criterion involving F_{12} explicitly in terms of uniaxial strengths. Tsai and Hahn (1980) suggest that, in the absence of other data, we should use $F_{12} = -0.5\sqrt{F_{11}F_{22}}$. Figure 12.13 shows the variation of strength with orientation assuming $F_{12} = 0$ for

the boron/epoxy system (Pipes and Cole 1973). The intrinsic properties of this boron fiber/epoxy system used to obtain the curve in Fig. 12.13 are as follows:

$$X_1^T = 27.3\,\text{MPa} \quad X_2^T = 1.3\,\text{MPa} \quad S = 1.4\,\text{MPa}$$
$$X_1^C = 52.4\,\text{MPa} \quad X_2^C = 6.5\,\text{MPa}$$

Note the excellent agreement between the computed curve using the quadratic interaction criterion and the experimental values. The agreement with the maximum stress criterion (dashed curve) is poor.

12.5.4.4 Comparison of Failure Theories

Important attributes of the four main failure theories, namely, maximum stress, maximum strain, maximum work, and quadratic interaction are compared in Table 12.1. The applicability of a given theory depends on material properties and the failure modes (Daniel and Ishai 1994). As expected, the maximum stress and maximum strain criteria are generally valid with brittle materials. They do require three subcriteria but are conceptually quite simple and experimental determination of parameters is also quite simple and straightforward. The two interactive theories, maximum work and quadratic interaction, are more suitable for computational purposes. In particular, the quadratic interaction criterion is quite general and comprehensive. Both require more complicated experimental characterization. According to Daniel and Ishai (1994), when material behavior and failure modes are not known and when a conservative approach is required, all four criteria should be evaluated

Table 12.1 Comparison of failure theories [after Daniel and Ishai (1994)]

Criterion	Physical basis	Computational aspects	Experimental characterization
Maximum stress	Tensile behavior of brittle material, no stress interaction	Inconvenient	Simple
Maximum strain	Tensile behavior of brittle material, no stress interaction	Inconvenient	Simple
Maximum work	Valid for ductile anisotropic materials, curve fitting for heterogeneous brittle composites	Can be programmed, different functions required for tensile and compressive strengths	Biaxial testing needed
Quadratic interaction	Mathematically consistent, reliable curve fitting	Simple, comprehensive	Complicated, numerous parameters needed

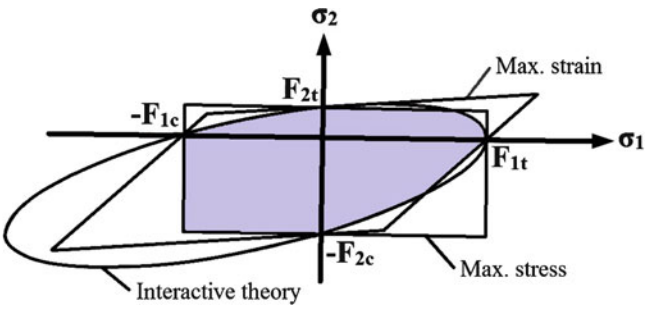

Fig. 12.15 Failure envelopes due to different failure criteria. The *shaded part* indicates the conservative failure region [after Daniel and Ishai (1994)]

and use the most conservative envelope in each quadrant. Figure 12.15 shows the four criteria in two-dimensional stress space. The shaded part of the envelopes conforms to this conservative approach.

References

Anand K, Gupta V, Dartford D (1994) Acta Metall Mater 42:797
Arsenault RJ, Fisher RM (1983) Scripta Metall 17:67
Budiansky B, Fleck N (1993) J Mech Phys Solids 41:183
Chawla KK (1973a) Metallography 6:155
Chawla KK (1973b) Philos Mag 28:401
Chawla KK (2003) Ceramic matrix composites, 2nd edn. Kluwer, Boston, MA
Chawla KK, Metzger M (1972) J Mater Sci 7:34
Chawla KK, Singh J, Rigsbee JM (1986) Metallography 19:119
Coleman BD (1958) J Mech Phys Solids 7:60
Cooper GA (1970) J Mater Sci 5:645
Cooper GA, Kelly A (1967) J Mech Phys Solids 15:279
Cottrell AH (1964) Proc R Soc 282A:2
Cowin SC (1979) J Appl Mech 46:832
Daniel IM, Ishai O (1994) Engineering mechanics of composite materials. Oxford University Press, New York, p 126
Daniels HE (1945) Proc R Soc A183:405
Dève HE (1997) Acta Mater 45:5041
Ebert LI, Gadd JD (1965) In: Fiber composite materials. ASM, Metals Park, OH, p 89
Gupta V, Anand K, Kryska M (1994) Acta Metall Mater 42:781
Grape J, Gupta V (1995a) Acta Metall Mater 43:2657
Grape J, Gupta V (1995b) J Compos Mater 29:1850
Hale DK, Kelly A (1972) Ann Rev Mater Sci 2:405
Hancox NL (1975) J Mater Sci 10:234
Hoffman O (1967) J Compos Mater 1:200

Kelly A (1970) Proc R Soc London A319:95
Kelly A (1971) In: The properties of fibre composites. IPS Science & Technology, Guildford, p 5
Kelly A, Lilholt H (1969) Philos Mag 20:311
Kyriakides S, Arseculeratne R, Perry EJ, Liechti KM (1995) Int J Solids Struct 32:689
Lager JR, June RR (1969) J Compos Mater 3:48
Narayanan S, Schadler LS (1999) Compos Sci Technol 59:2201
Outwater JO, Murphy MC (1969) In: Proceedings of the 24th SPI/RP conference, paper 11–6, Society of Plastics Industry, New York
Piggott MR (1984) In: Developments in reinforced plastics, 4th edn. Elsevier Applied Science Publishers, London, p 131
Piggott MR, Harris B (1980) J Mater Sci 15:2523
Pipes RB, Cole BW (1973) J Compos Mater 7:246
Rosen BW (1965a) In: Fiber composite materials. American Society for Metals, Metals Park, OH, p 58
Rosen BW (1965b) In: Fiber composite materials. American Society for Metals, Metals Park, OH, p 37
Rosen BW (1983) In: Mechanics of composite materials: recent advances. Pergamon, Oxford, p 105
Rowlands RE (1985) Failure mechanics of composites, vol 3 of the series handbook of composites. North-Holland, Amsterdam, p 71
Saghizadeh H, Dharan CKH (1985) American Society of Mechanical Engineering. Paper #85WA/Mats-15, presented at the Winter Annual Meeting, Miami Beach, FL
Schultheisz CR, Waas AM (1996) Prog Aerospace Sci 32:1
Tsai SW, Hahn HT (1980) Introduction to composite materials. Technomic, Westport, CT
Tsai SW, Wu EM (1971) J Compos Mater 5:58
Vogelsang M, Arsenault RJ, Fisher RM (1986) Metall Trans A 17A:379
Waas AM, Schultheisz CR (1996) Prog Aerospace Sci 32:43
Zweben C, Rosen BW (1970) J Mech Phys Solids 18:189

Further Reading

Daniel IM, Ishai O (2006) Engineering mechanics of composite materials, 2nd edn. Oxford University Press, New York
Nahas MN (1986) J Comp Technol Res 8:138

Problems

12.1. For a ceramic fiber with $\mu = 12\ \%$, show that $\beta \approx 10$. Show also that if the fiber length is changed by an order of magnitude, the corresponding drop in the average strength is about 20 %.

12.2. In a series of tests on boron fibers, it was found that $\mu = 10\ \%$. Compute the ratio $\overline{\sigma}_B/\overline{\sigma}$, where $\overline{\sigma}_B$ is the average strength of the fiber bundle and $\overline{\sigma}$ is the average strength of fibers tested individually.

12.3. Estimate the work of fiber pullout in a 40 % carbon fiber/epoxy composite. Given $\sigma_{fu} = 0.2$ GPa, $d = 8$ μm, and $\tau_i = 2$ MPa.

12.4. How would you go about testing a single fine-diameter fiber (recall that carbon fiber has a diameter of about 7 μm)? Do discuss the effect of variability in diameter of the fiber along its length in computing the strength of the fiber.